

Implications of new early *Homo* fossils from Ileret, east of Lake Turkana, Kenya.
F. Spoor, M. G. Leakey, P.N. Gathogo, F.H. Brown, S.C. Antón, I. McDougall, C. Kiarie, F.K. Manthi, and L.N. Leakey

Contents

1. Measurements & comparisons
 - 1.1. KNM-ER 42700. Calvarial measurements
 - 1.2. KNM-ER 42703. Dental and palatal measurements
 - 1.3. Summary of morphological features used in the differential diagnoses
2. Morphometric analyses
 - 2.1. KNM-ER 42700.
 - 2.1.1. Principal component analysis
 - 2.1.2. Bivariate analyses
 - 2.1.3. Analysis of intraspecific variation
 - 2.2. KNM-ER 42703. Principal component analysis
3. Last known occurrence of *Homo habilis* at Lower Bed II, Olduvai
4. References

General notes related to the tables

Definitions of measurements indicated by Martin #¹, and Wood #². All linear measurements given in millimeters, and volumes in cm³. Estimated measurements in brackets. Dental measurements corrected for interstitial wear, but not occlusal wear.

Homo erectus, three samples considered (adults):

- a. Africa: Turkana Basin, Olduvai, Olorgesailie, Daka.
- b. Earlier: Africa plus Dmanisi, Sangiran, and Trinil.
- c. All: Earlier plus Ngandong, Ngawi, Sambungmacan, Hexian, Nanjing, and Zhoukoudian.

Homo habilis (*sensu stricto*, adults): Olduvai, Turkana Basin (incl Omo L894-1, but not KNM-ER 1470, 3732).

Comparative measurements were either taken by FS and SCA, or obtained from the literature, with main sources listed as Refs 2-17 (full information available on request from FS).

NB: Our early *Homo* hypodigms broadly follow Refs 2 and 7, and differ distinctly from the interpretation of Ref 4, in which KNM-ER 1470 and OH 65 are affiliated with the *H. habilis* type OH 7, to the exclusion of OH 13, OH 24, OH 62, and KNM-ER 1813. In our view OH 65 is best attributed to *H. habilis*, and lacks the derived maxillary morphology of the *H. rudolfensis* lecto type KNM-ER 1470 (see main text).

1. Measurements & comparisons

1.1. KNM-ER 42700. Calvarial measurements of KNM-ER 42700, compared with *H. erectus* (2 juveniles given separately), and *H. habilis*.

	Endocran volume	Max. length (g-op)	Basion bregma height	Porion vertex height	Bi-auricular breadth	Max. breadth	Glabella bregma chord	Glabella bregma arc	Supraorb. torus thickness	Sup. facial breadth	Postorb. breadth	Parietal sagittal chord	Parietal sagittal arc
Martin # ¹	M38	M1	M17	M21	M11	M8	M29d	M26a	-	M43	M9(1)	M30	M27
Wood # ²	-	W1	W4	W6	-	-	W17	W18	W62	W49	W8	W25	W26
KNM ER 42700	691	[153]	94	87	110	120	[95]	[100]	7	96	79	87	94
<i>H. erectus</i> (Africa) n	4	4	4	4	4	4	4	4	8	3	5	3	3
mean	909	188	111	96	134	143	103	110	12	125	90	86	92
min	727	180	101	91	130	139	95	101	8	119	78	79	83
max	1067	206	121	102	140	150	120	128	19	136	100	94	99
SD	151.9	12.4	8.2	5.2	4.4	4.8	11.4	12.3	4.1	9.5	8.3	7.5	8.1
<i>H. erectus</i> (earlier) n	13	10	6	9	12	13	9	9	13	6	13	13	13
mean	884	184	110	95	134	143	101	106	12	120	89	92	97
min	655	163	101	90	120	132	87	90	8	104	78	79	83
max	1067	207	121	104	149	161	120	128	19	136	101	107	111
SD	126.7	15.0	7.1	5.8	8.0	7.7	11.3	11.9	3.6	10.5	7.4	7.4	7.7
<i>H. erectus</i> (all) n	31	28	10	25	27	28	26	24	31	13	26	33	33
mean	979	192	114	100	139	147	105	111	14	116	94	96	102
min	655	163	101	90	120	132	87	90	8	104	78	79	83
max	1251	219	124	112	152	161	120	128	20	136	110	109	115
SD	145.5	13.1	7.8	6.9	8.6	7.1	8.6	9.0	3.1	8.4	8.9	7.3	7.9
KNM-WT 15000 (juv.)	880	[175]	109	91	126	141	[90]	[94]	[13]	112	91	99	107
D2700 (juv.)	~ 600	155	101	77	119	126	84	88	8	96	[77]	87	91
<i>H. habilis</i> n	3	2	2	3	2	3	2	2	2	2	3	3	3
mean	562	146	93	78	115	120	83	91	8	100	77	78	83
min	509	145	90	77	112	113	77	85	6	100	69	75	79
max	594	147	95	79	118	128	89	96	9	100	88	82	87
SD	46.0	1.1	3.7	1.2	4.2	7.5	8.5	7.8	2.1	0.0	9.8	3.6	4.0

1.1. Continued

	Occipital sagittal chord	Occipital sagittal arc	Lambda inion chord	Inion opisthion chord	Occipital angle	Bi-asterionic breadth	Mand. fossa breadth	Bregma thickness parietal	Lambda thickness parietal	Parietal eminence thickness	EOP** thickness
Martin# ¹	M31	M28	M31(1)	M31(2)	M33d	M12	-	-	-	-	-
Wood# ²	W39	W40	W35	W37	OCA16	W41	W82	W106	W107	W111	W115
KNM ER 42700	74	92	54, 47*	29, 39*	114	99	20	4	7	5	9
<i>H. erectus</i> (Africa) n	5	5	7	5	2	6	3	6	6	7	9
mean	83	108	50	47	109	119	29	8	9	8	16
min	75	91	38	38	102	110	26	7	7	7	12
max	95	122	61	52	115	124	32	10	10	10	21
SD	8.3	12.4	7.2	5.9	9.2	5.2	3.1	1.0	1.2	1.5	2.8
<i>H. erectus</i> (earlier) n	12	12	16	11	7	16	6	16	12	16	18
mean	81	107	49	48	105	116	28	8	9	9	17
min	72	91	38	38	91	99	24	6	7	7	10
max	95	122	61	56	117	138	32	11	13	12	30
SD	6.3	10.7	5.6	4.9	9.0	10.3	2.8	1.4	2.0	1.5	4.5
<i>H. erectus</i> (all) n	26	25	30	22	19	36	18	34	23	24	31
mean	83	111	52	51	103	119	23	9	10	10	18
min	72	91	38	38	91	99	17	6	7	7	10
max	95	127	66	65	117	142	32	12	13	16	30
SD	5.2	9.9	6.1	6.7	6.7	9.9	5.3	1.4	1.9	2.2	4.5
KNM-WT 15000 (juv.)	76	91	44	42	118	106	25	8.2	6.1	5	10.4
D2700 (juv.)	[70]	[87]	45	39	115.6	105	-	-	-	-	-
<i>H. habilis</i>	2	2	3	2	2	3	2	3	3	3	3
mean	73	91	46	35	117	90	27	5	6	6	13
min	70	87	39	34	114	80	26	4	4	5	10
max	75	95	55	35	120	96	27	6	7	7	17
SD	3.5	5.7	8.1	0.7	4.2	8.5	0.7	1.0	1.5	1.0	3.8

* inion far anteriorly on nuchal plane (as in Daka³). First value to inion, second value to a point more posteriorly best marking the division between upper and lower scales of the occipital, equivalent to values given for published specimens.

** External occipital protuberance

1.2. KNM-ER 42703. Dental and palatal measurements of KNM-ER 42703, compared with *H. habilis* and *H. erectus*. Values of KNM-ER 42703 compensate for a few fine cracks in the crowns of P⁴ to M³.

		C, MD	C, LL	P ³ MD	P ³ BL	P ⁴ MD	P ⁴ BL	M ¹ MD	M ¹ BL	M ² MD	M ² BL	M ³ MD	M ³ BL	Palatal length	Palatal breadth	Palatal depth
Martin # ¹														62	63	64
Wood # ²		190	191	193	194	202	203	211	212	223.0	224	235	236			
KNM-ER 42703		>9.0	>9.5	9.0	>12.0	8.8	12.4	12.6	13.3	13.0	14.1	12.5	14.1	[57]	[43]	[10]
<i>H. habilis</i>	n	5	5	8	8	8	8	13	13	8	8	8	8	4	4	4
	mean	9.2	9.5	9.0	11.9	9.2	11.9	12.9	13.0	12.9	14.2	12.6	14.6	55	38	12
	min	8.2	8.5	8.1	11.1	8.5	11.2	11.6	12.0	11.8	13.5	11.3	13.4	50	32	6
	max	10.0	10.2	9.8	12.7	9.9	13.1	14.7	14.1	13.5	16.4	13.9	16.7	59	45	17
	SD	0.77	0.64	0.62	0.65	0.47	0.64	0.86	0.62	0.65	0.93	0.98	1.25	4.1	6.5	4.5
<i>H. erectus</i> (Africa)	n	1	1	3	3	2	2	3	2	3	3	3	3			
	mean	9.6	10.2	8.8	12.2	8.2	11.9	12.6	12.9	12.2	13.4	9.6	11.2			
	min			8.6	11.8	8.1	11.8	12.2	12.2	11.7	12.7	7.8	9.9			
	max			9.1	12.8	8.3	12.1	13.0	13.6	13.1	14.2	11.4	12.9			
	SD			0.29	0.53	0.14	0.25	0.40	0.99	0.78	0.75	1.79	1.56			
<i>H. erectus</i> (earlier)	n	8	9	17	16	11	12	15	14	14	14	15	15			
	mean	10.0	10.2	8.2	11.4	7.8	11.2	12.2	13.0	12.2	13.1	10.2	12.6			
	min	9.0	9.2	7.1	9.9	6.8	10.0	11.0	11.0	10.6	10.9	7.8	9.9			
	max	11.1	11.8	9.1	12.8	8.3	12.4	13.6	14.2	13.6	15.4	12.7	15.3			
	SD	0.62	0.80	0.60	0.93	0.49	0.88	0.72	0.82	0.93	1.20	1.29	1.67			
<i>H. erectus</i> (all)	n	14	15	22	21	21	22	22	20	23	23	22	22	4	4	4
	mean	9.7	10.2	8.3	11.5	8.0	11.4	12.0	12.9	11.9	13.1	10.0	12.3	57	42	16
	min	8.5	9.2	7.1	9.9	6.8	10.0	10.1	11.0	10.3	10.9	7.8	9.9	50	34	13
	max	11.1	11.8	9.2	12.8	9.0	13.4	13.6	14.2	13.6	15.5	12.7	15.3	70	50	20
	SD	0.67	0.64	0.62	0.93	0.59	0.89	0.87	0.82	0.96	1.14	1.13	1.50	8.8	7.1	3.3

1.3. Summary of morphological features used in the differential diagnosis of KNM-ER 42700 and KNM-ER 42703

Character	<i>H. erectus</i>	KNM-ER 42700	<i>H. habilis</i>	KNM- ER 42703	<i>H. rudolfensis</i> (KNM-ER 1470)
Frontal keeling	variable	yes	no	-	no
Parietal keeling	variable	yes	no	-	no
TMJ mediolaterally narrow*	yes	yes	no	-	no
Tympanic-petrous angled	yes	yes	no	-	?
Upper scale occipital relatively low*	yes	yes	no	-	no
Opisthocranium high on occipital profile	yes	yes	no	-	no
Upper molar size*	smaller	-	larger	larger	?
M ² & M ³ outline	rhomboidal	-	variable	rectangular	?
M ³ mesiodistal shortened*	yes	-	no	no	?

* Importance of character shown quantitatively by loadings in principal component analyses (Suppl. Notes 2.1.1 & 2.2)

Character states based on original observations by the authors, and on reviews in Refs. 2, 9, 18.

Calvarial characters found not to discriminate between *H. habilis* and *H. erectus*, when scaling effects are taken into account include supraorbital torus thickness, vault thickness at the parietal boss, and midsagittal curvature of the occipital (see Suppl. Note 2.1.2).

2. Morphometric analyses

2.1. KNM-ER 42700.

2.1.1a Method. Principal component analysis of 10 calvarial measurements listed in the results table below (PAST v1.59)¹⁹. To correct for overall size each measurement was divided by the geometric mean of the 10 measurements. Lambda-inion and inion-opisthion chord values used for KNM-ER 42700 are 47 and 39, respectively (see footnote Suppl Note 1.1).

2.1.1b. Comparative samples:

Homo erectus: KNM-ER 3733, KNM-ER 3883, OH 9, D2280, San 17, Ng 1, Ng 6, Ng 7, Ng 11, Ng 12, Ngawi, Sm 3, ZHD III, ZHD XI, ZHD XII. Juveniles: D2700, KNM-WT 15000.

Homo habilis: KNM-ER 1813

Homo rudolfensis: KNM-ER 1470

2.1.1c. Results.

	PC1	PC2	PC3	PC4	PC5	PC6
Eigenvalue	0.022	0.010	0.006	0.005	0.004	0.002
% variance	42	19	12	10	7	5
Loadings:						
Max. length (g-op)	0.554	-0.269	0.062	-0.072	0.040	-0.113
Porion-vertex height	0.230	0.189	0.367	-0.248	-0.336	-0.089
Max breadth	0.270	0.198	0.026	0.010	0.406	-0.782
Glabella-bregma chord	0.329	-0.094	-0.113	-0.030	-0.699	-0.092
Parietal sagittal chord	0.267	0.743	-0.272	-0.253	0.125	0.367
-						
Lambda-inion chord	0.234	0.109	0.659	0.101	-0.103	0.019
Inion-opisthion chord	0.280	-0.511	-0.026	-0.212	0.346	0.357
-						
Occipital sagittal chord	0.110	0.034	0.404	-0.257	0.272	0.104
Bi-asterionic breadth	0.296	0.120	0.099	0.862	0.098	0.212
-						
Mand. fossa breadth	0.392	-0.056	-0.409	0.074	-0.056	-0.204

2.1.1d. Conclusions. A plot of PC3 against PC1 (Fig 2a, main article) shows that KNM 1813 (*H. habilis*) and KNM-ER 1470 (*H. rudolfensis*) are significantly different from *H. erectus* along PC1. The loadings indicate that this particularly reflects that *H. erectus* has a relatively smaller mandibular fossa breadth and upper occipital scale height (lambda-inion chord). KNM-ER 42700 falls within the convex hull and 95% confidence ellipse of adult *H. erectus*, and away from KNM 1813 and KNM-ER 1470. Along PC3 the juvenile *H. erectus* specimens KNM-ER 15000 and D2700 fall lower than most adult *H. erectus*. In contrast, KNM-ER 42700 groups with the adults, suggesting that most or all of growth reflected in PC3 had been achieved. Such a conclusion is supported by the advanced fusion of the sphenoccipital synchondrosis. PC2 reflects, among others, midline occipital curvature. This feature scales allometrically in *H. erectus*, and does not separate this species from *H. habilis* (Suppl. Note 2.1.2).

2.1.2. Bivariate analyses of the supraorbital torus thickness and vault thickness at the parietal eminence against endocranial volume, and of occipital midsagittal chord against arc.

2.1.2a samples

Supraorbital torus thickness:

Homo erectus: KNM-ER 3733, KNM-ER 3883, OH 9, OH 12, Daka BOU-VP-2/66, D2280, D2282, D3444, San 2, San 17, Ng 1, Ng 6, Ng 7, Ng 10, Ng 11, Ng 12, Ngawi 1, Sm 1, Sm 3, Sm 4, Hexian PA830, Nanjing 1, ZHD-II, ZHD-III, ZHD-X, ZHD-XI, ZHD-XII. Juveniles: KNM-WT 15000, D2700, Mojokerto.

Homo rudolfensis: KNM-ER 1470

Homo habilis: KNM-ER 1813, OH 24

Parietal eminence thickness:

Homo erectus: KNM-ER 3733, KNM-ER 3883, OH 9, OH 12, San 2, San 4, San 10, San 12, San 17, Trinil2, Sm 3, Hexian PA830, ZHD-II, ZHD-III, ZHD-X, ZHD-XI, ZHD-XII. Juvenile: KNM-WT 15000.

Homo rudolfensis: KNM-ER 1470

Homo habilis: KNM-ER 1805, KNM-ER 1813, OH 24. Juveniles: OH 7, OH 13, OH 16

Occipital curvature (arc - chord):

Homo erectus: KNM-ER 730, KNM-ER 3733, KNM-ER 3883, OH 9, Daka BOU-VP-2/66, D2280, D3444, San 2, San 4, San 12, San 17, Skull IX, Ng 1, Ng 6, Ng 7, Ng 10, Ng 11, Ng 12, Ngawi 1, Sm 3, Sm 4, Hexian PA830, ZHD-III, ZHD-XI, ZHD-XII. Juveniles: KNM-WT 15000, D2700, Mojokerto.

Homo rudolfensis: KNM-ER 1470

Homo habilis: KNM-ER 1813, OH 24. Juvenile: OH 13.

2.1.2b Methods

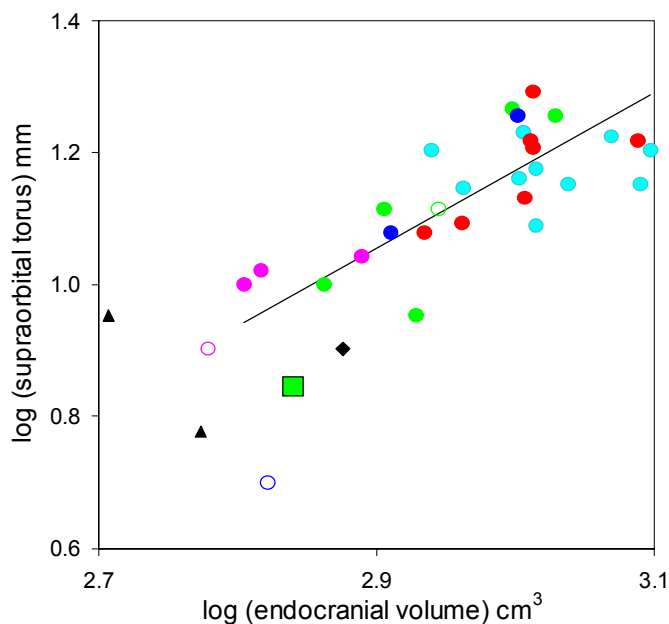
Measurements as defined in Ref.2 (# 62, 111, 39, 40).

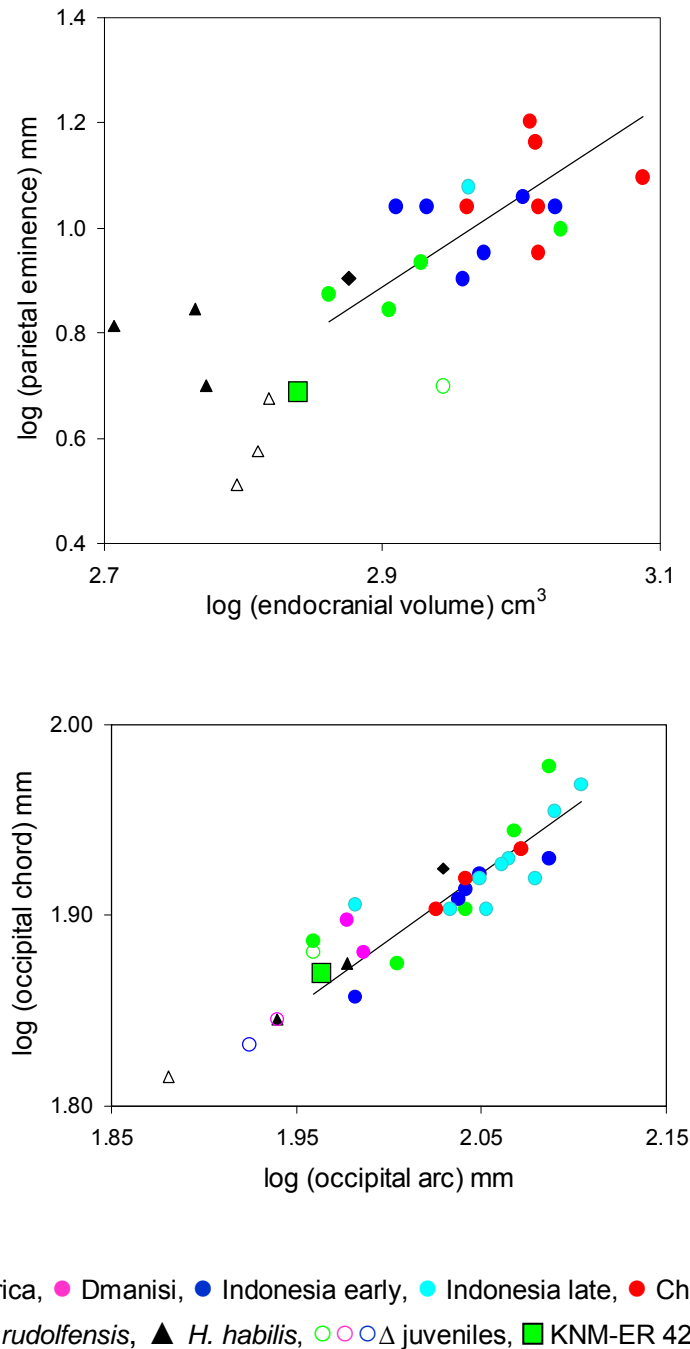
Calculation of Spearman's rank correlation coefficients and tests for allometry, that is whether the slope of the double log regression differs significantly from 1 (linear measurements) or 0.33 (linear measurement against endocranial volume), were done with PAST v1.59¹⁹. The reduced major axis (RMA) regression of the adult *H. erectus* sample was used to predict values for KNM-ER 42700, and the actual values of this specimen were compared with the 95% confidence intervals of the predicted values (calculated in Ms Excel 2003).

2.1.2c Results

x:		Endocranial volume		Endocranial volume		Occipital sagittal arc (#31)	
y:		Supraorbital torus thickness (#62)		Parietal eminence thickness (#111)		Occipital sagittal chord (#39)	
<i>Homo erectus</i> (all)	n	27		17		25	
	r_{rank}	0.622 Xxx		0.516 x		0.891 xxx	
Allometry / Isometry		A		A		A	
RMA slope, +/- 95%		1.178 0.333		1.719 0.771		0.697 0.160	
Int.		-2.361		-4.099		0.494	
		log	raw	log	raw	log	raw
KNM-ER 42700, x observed		2.84	691	2.84	691	1.96	92
KNM-ER 42700, y predicted		0.98	10	0.78	6	1.86	73
SE of y predicted		0.07		0.10		0.02	
	-95%	0.84 7		0.58 4		1.83 67	
	95%	1.13 13		0.99 10		1.90 79	
KNM-ER 42700, y observed			7		5		74
In predicted range?			Y		Y		Y

Bivariate double logarithmic plots of supraorbital torus thickness, vault thickness at the parietal eminence, and occipital curvature (midsagittal chord to arc). Adult *Homo erectus* is represented by the first five symbols of the legend, and open symbols mark juveniles of the particular groups. The relationships in adult *H. erectus* is indicated by the reduced major axis.





2.1.2d Conclusions:

In the adult *H. erectus* sample the supraorbital torus and parietal eminence thicknesses are correlated with overall calvarial size, as indicated by endocranial volume (used instead of external measurements to exclude vault thickness). Both scale positively allometrically, that is the slope of the log-log plot is significantly larger than the 0.33, representing isometry. This allometric scaling implies that the torus and vault thicknesses increase disproportionately with larger calvarial size. The occipital chord scales negatively allometrically to the arc (slope <1), implying that larger specimens of *H. erectus* tend to have less rounded, more angulated occipitals. KNM-ER 42700 is not significantly different from these trends.

2.1.3 Comparisons of the intraspecific variation of calvarial dimensions between *H. erectus*, and modern *H. sapiens*, *Pan troglodytes* and *Gorilla gorilla*.

2.1.3a Samples

Homo erectus calvarial length (g-op)

KNM ER 42700, KNM-ER 3733, KNM-ER 3883, OH 9, Daka BOU-VP-2/66, D2280, D2282, D3444, San 2, San 17, Skull IX, Trinil2, Ng 1, Ng 6, Ng 7, Ng 10, Ng 11, Ng 12, Ngawi 1, Sm 1, Sm 3, Sm 4, Hexian PA830, Nanjing 1 Tang shan, ZHD-II, ZHD-III, ZHD-V, ZHD-X, ZHD-XI, ZHD-XII.

Homo erectus calvarial height (ba-br)

KNM ER 42700, KNM-ER 3733, KNM-ER 3883, OH 9, Daka BOU-VP-2/66, D2280, D2282, San 17, Ng 1, Ng 6, Ng 7, Ng 10, Ng 12, Ngawi 1, Sm 4.

Homo erectus calvarial breadth (bi-au)

KNM ER 42700, KNM-ER 3733, KNM-ER 3883, OH 9, Daka BOU-VP-2/66, D2280, D2282, D3444, San 2, San 4, San 10, San 12, San 17, Skull IX, Ng 6, Ng 7, Ng 10, Ng 11, Ng 12, Ngawi 1, Sm 1, Sm 3, Hexian PA830, Nanjing 1 Tang shan, ZHD-III, ZHD-V, ZHD-X, ZHD-XI, ZHD-XII

Homo sapiens: A geographically diverse, mixed sex sample housed in the Department of Anatomy & Developmental Biology, UCL, London (U.K.), and the full Howells data set²⁰ representing a large (n=2524) geographically diverse, mixed sex sample

Pan troglodytes: 22 males, 26 females, mixed subspecies

Collections of the Powell Cotton Museum, Birchington, and the Department of Anatomy & Developmental Biology, UCL, London (U.K.).

Gorilla gorilla: 25 males, 21 females, mixed subspecies

Collections of the Powell Cotton Museum, Birchington, and the Department of Anatomy & Developmental Biology, UCL, London (U.K.).

2.1.3b Methods

The calvarial dimensions examined are overall length (glabella – opisthocranium), basion – bregma height and bi-auricular breadth. The latter two were used, rather than porion-vertex height and maximum cranial breadth, respectively, because they are more homologous when comparing hominin and great ape cranial shapes.

The Howells data set was used in parallel with the UCL *H. sapiens* sample specifically measured for this study, thus providing an independent control of the results for this species based on a much larger sample. Note that the Howells dataset provides measurements of bi-radicular breadth rather than bi-auricular breadth, but in *H. sapiens* these landmarks are very close, and variation in the measure rather than the actual measurements are compared here.

For the small samples of fossil taxa coefficients of variation (CV) are likely biased, and the reported values were therefore sample size corrected using the parameter V^* , calculated as: $(1 + 1/[4n]) * SD/mean^{21}$.

The degree of intraspecific variation of the three *H. erectus* samples are compared with that of the modern hominid samples by resampling of the CV with bootstrapping methodology^{22, 23}. For each comparison 5000 random samples of a modern group were drawn with replacement at a sample size equivalent to that of the *H. erectus* sample. The CV of the *H. erectus* sample was then compared to the simulated distribution of CVs for the comparative sample to determine the likelihood that the former could be sampled from the latter. To avoid the probability of $p = 0$ it is reported as $p = (P+1)/(5000+1)$. P is the number of random modern samples whose CV exceeds or is equal to that of the *H. erectus* sample (hypothesis that the modern CV is smaller than that of *H. erectus*), or whose CV is smaller or equal to that of the *H. erectus* sample (hypothesis that the modern CV is larger than that of *H. erectus*). The null hypothesis in a one-tailed test that the CV of the *H. erectus* sample is either not significantly larger or smaller than that of the modern sample is rejected at $p \leq 0.05$. All calculations were done in MS Excel 2003.

2.1.3c Results

	<i>Homo erectus</i>			<i>Homo sapiens</i>		<i>Pan troglodytes</i>	<i>Gorilla gorilla</i>
	Africa	early	all	Howells	this study		
LENGTH							
n	5	12	30	2524	57	48	46
CV (V*)	10.4	9.0	7.6	4.8	5.1	3.9	14.2
p, Africa				0.0002 >	0.0002 >	0.0002 >	0.2583 =
p, early				0.0002 >	0.0002 >	0.0002 >	0.0242 <
p, all				0.0002 >	0.0002 >	0.0002 >	0.0002 <
HEIGHT							
n	5	8	15	2524	57	48	46
CV (V*)	9.5	9.5	10.1	5.5	4.9	5.4	11.0
p, Africa				0.0120 >	0.0014 >	0.0062 >	0.3219 =
p, early				0.0028 >	0.0002 >	0.0002 >	0.2549 =
p, all				0.0002 >	0.0002 >	0.0002 >	0.3019 =
BREADTH							
N	5	14	29	2524	57	48	46
CV (V*)	8.7	7.4	7.3	6.1	6.1	4.9	10.8
p, Africa				0.0944 =	0.0826 =	0.0004 >	0.2909 =
p, early				0.1286 =	0.1194 =	0.0002 >	0.0226 <
p, all				0.0716 =	0.0612 =	0.0002 >	0.0004 <

>, <, =: Compared with the extant species the *H. erectus* sample has a CV that is larger, smaller or not significantly different, respectively. $p = 0.0002$ equals $p = (0+1)/(5000+1)$, the result when no CV of an extant sample among the 5000 random draws is equal to, or either larger or smaller (depending on hypothesis) than the *H. erectus* sample.

2.1.3d Conclusions.

Overall *H. erectus* is more variable in calvarial dimensions than *H. sapiens* and *P. troglodytes*, but less variable than *G. gorilla*. However, *H. erectus* does not differ significantly in its variation of breadth from *H. sapiens*, and variation of height from *G. gorilla*. The variation of all three dimensions within the African *H. erectus* sample, visually demonstrated below, is not significantly different from that of *G. gorilla*.



Superior view of KNM-ER 42700 (left) and OH 9 (right), demonstrating the size difference between the smallest and largest of the African specimens attributed to *H. erectus* (scale bar 5 cm; image of OH 9 by J. Reader)

2.2. KNM-ER 42703

2.2a. Method. Principal component analysis of mesiodistal (MD) and buccolingual (BL) dimensions of M¹ to M³ (PAST v1.59)¹⁹.

2.2b. Comparative samples:

Homo erectus: KNM-WT 15000, D2700, San 4, San 7-3a-d, San 17, Skull IX, ZKD L2-99, ZKD O1-313

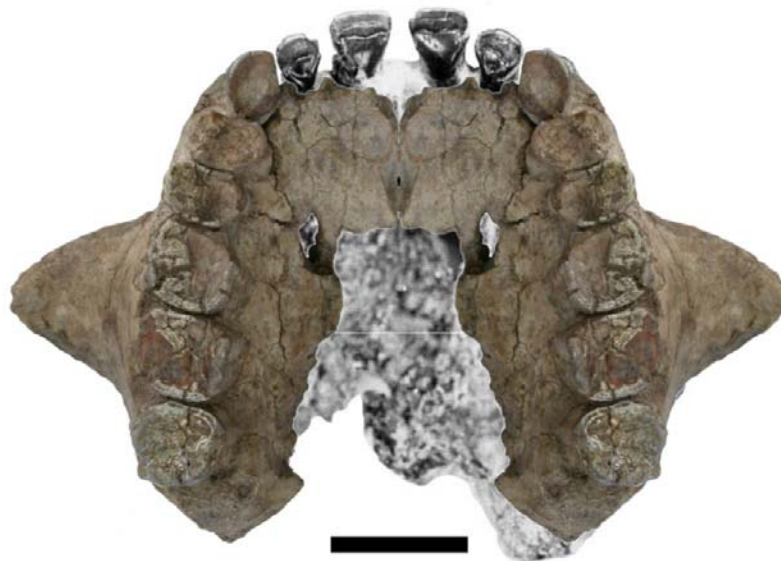
Homo habilis: KNM-ER 1805B, KNM-ER 1813, Omo L894-1, OH 13, OH 16, OH 24, OH 65

H. aff. habilis: Stw 53 (shown in Figure 2b, but not included in the *H. habilis* sample).

2.2c. Results.

	PC1	PC2	PC3	PC4	PC5	PC6
Eigenvalue	8.802	1.254	0.752	0.262	0.145	0.057
% variance	78	11	7	2	1	1
Loadings:						
M ¹ MD	0.252	0.716	-0.183	-0.619	0.061	-0.064
M ¹ BL	0.218	0.040	0.212	0.100	-0.541	-0.777
M ² MD	0.290	0.526	0.117	0.623	-0.267	0.407
M ² BL	0.376	0.020	0.643	0.066	0.645	-0.158
M ³ MD	0.559	-0.179	-0.681	0.270	0.283	-0.200
M ³ BL	0.593	-0.421	0.176	-0.375	-0.371	0.402

2.2d. Conclusions. a plot of PC3 against PC1 (Figure 2b of main article) separates *H. erectus* and *H. habilis* specimens, with the former having smaller molars overall, and a mesiodistally shorter M³ in particular. KNM-ER 42703 falls within the convex hull and 95% confidence ellipse of *H. habilis*, but outside those of *H. erectus*.



Inferior view of KNM-ER 42703, combined with mirror-imaged left side, and superimposed on OH 65, a *H. habilis* maxilla with very similar palatal size (scale bar 2 cm; OH 65 in grey scale after Ref 4).

3. Last known occurrence of *Homo habilis* at Lower Bed II, Olduvai

Previously the last occurring, definitive member of *H. habilis* (OH 13) is from lower Bed II at Olduvai Gorge, Tanzania. Portions of OH 13 were found *in-situ* at geological locality 88, archaeological site 71a (MNK)²⁴. Excavations place OH 13 below the Lemuta member and about 2 m below Tuff IIB, and above tuffs IIA and IF^{24,25}. Due to the mostly reworked nature of Bed II tuffs²⁵, the age of OH 13 is not as well constrained as its stratigraphic position. Its oldest possible age is 1.78 Ma as defined by the top of the Olduvai normal event which coincides with the transition between beds I and II²⁶, and is corroborated by ⁴⁰Ar/³⁹Ar dates on Tuff IF at the top of Bed I²⁷. The overlying Tuff IIB is not dated, but the closely positioned, but underlying Tuff IIA yielded a not very well constrained ⁴⁰Ar/³⁹Ar age of 1.66 Ma²⁸ and ref.25 argued in favor of an age of 1.6 Ma for the overlying Lemuta Member. The top of Bed II (some 25 m higher in the section than OH 13) is estimated to date to 1.47 Ma based on ⁴⁰Ar/³⁹Ar dates for Tuff IID²⁸. Given these data points, an age for OH 13 is likely to be about 1.65 Ma and no older than 1.78 Ma.

4. References

1. Bräuer, G. Osteometrie. in *Anthropologie: Handbuch der Vergleichenden Biologie des Menschen*. (Eds. Martin, R. and Knussmann R.) 160–232. (Gustav Fischer, Stuttgart, 1988)
2. Wood, B. *Koobi Fora Research Project Vol. 4: Hominid Cranial Remains*. (Clarendon Press, Oxford, 1991)
3. Asfaw, B. et al. Remains of *Homo erectus* from Bouri, Middle Awash, Ethiopia. *Nature* **416**, 317–320 (2002).
4. Blumenshine R. J. et al. Late Pliocene *Homo* and hominid land use from western Olduvai Gorge, Tanzania. *Science* **299**, 1217–1221 (2003).
5. Bromage, T.G., Schrenk, F., & Zonneveld, F.W. Paleoanthropology of the Malawi Rift: An early hominid mandible from the Chiwondo Beds, northern Malawi. *J. Hum. Evol.* **28**, 71–108 (1995).
6. Grine, F.E. and Franzen, J.L. Fossil hominid teeth from the Sangiran Dome (Java, Indonesia). *Courier Forsch. Senckenberg* **171**, 75–103 (1994).
7. Kimbel, W.H., Johanson, D.C. & Rak, Y. Systematic assessment of a maxilla of *Homo* from Hadar, Ethiopia. *Am. J. Phys. Anthropol.* **103**, 235–262 (1997).
8. Marquéz, S., Mowbray, K., Sawyer, G. J., Jacob, T. & Silvers, A. (2001). New fossil hominid calvaria from Indonesia—Sambungmacan 3. *Anat. Rec.* **262**, 344–368.
9. Rightmire, G.P. *The Evolution of Homo erectus*. Cambridge University Press, Cambridge (1990).
10. Rightmire, G.P., Lordkipanidze, D. & Vekua, A. Anatomical descriptions, comparative studies and evolutionary significance of the hominin skulls from Dmanisi, Republic of Georgia. *J. Hum. Evol.* **50**, 115–141 (2006).
11. Santa Luca, A.P. The Ngandong fossil hominids: a comparative study of a far eastern *Homo erectus* group. *Yale Univ. Publ. Anthropol.* **78**, 1–175 (1980).
12. Tobias, P.V. *Olduvai Gorge Volume 4: The Skulls and Endocasts of Homo habilis*. (Cambridge University Press, Cambridge, 1991).
13. Walker, A. C. & Leakey, R. E. F. *The Nariokotome Homo erectus Skeleton* (Harvard Univ. Press, Cambridge, Massachusetts, 1993).
14. Weidenreich F. The dentition of *Sinanthropus pekinensis*: a comparative odontography of the hominids. *Palaeontol. Sin. Ser.* **D1**, 1–180 (1937).
15. Weidenreich F. The skull of *Sinanthropus pekinensis*: a comparative study on a primitive hominid skull. *Palaeont. Sin. Ser.* **D10**, 1–298 (1943).

16. Widiyanto, H. and Zeitoun, V. Morphological description, biometry and phylogenetic position of the skull of Ngawi 1 (East Java, Indonesia). *Int. J. Osteoarchaeol.* **13**, 339-351 (2003).
17. Wu, X. and Poirier, F.E. *Human evolution in China: a metric description of the fossils and a review of the sites*. New York: Oxford University Press. (1995)
18. Antón, S.C. A Natural History of *Homo erectus*. *Yb. Phys. Anthropol.* **46**, 126–170 (2003).
19. Hammer Ø, Harper, D. A.T. and Ryan P. D. Past: paleontological statistics software package for education and data analysis. *Palaeontol. Electron.* **4**, 1-9 (2001).
20. Howell, W.W. Howells' craniometric data on the internet. *Am. J. Phys. Anthropol.* **101**, 441-442 (1996)
21. Sokal RR and Braumann CA. Significance tests for coefficients of variation and variability profiles. *Syst. Zool.* **29**, 50–66 (1980).
22. Lockwood, C.A., Richmond, B.G., Jungers, W.L., Kimbel, W.H.. Randomization procedures and sexual dimorphism in *Australopithecus afarensis*. *J. hum. Evol.* **31**, 537-548 (1996).
23. Lockwood, C.A., Kimbel, W.H., Johanson, D.C. Temporal trends and metric variation in the mandibles and dentition of *Australopithecus afarensis*. *J. hum. Evol.* **39**, 23-55 (2000).
24. Leakey, M.D. *Olduvai Gorge Volume 3: Excavations in Beds I and II, 1960–1963*. (Cambridge University Press, Cambridge, 1971).
25. Hay, R.L. *Geology of Olduvai Gorge*. (University of California Press, Berkeley, 1976).
26. Tamrat, E., Tohveny, N., Taieb, M. and Opdyke, N. Revised magnetostratigraphy of PlioPleistocene sedimentary sequence of the Olduvai formation (Tanzania). *Paleogeogr. Paleoclimatol. Paleoecol.* **114**, 273–283 (1995).
27. Walter, R.C., Manega, P. C., Hay, R. L., Drake, R. E. & Curtis, G. H. Laser-fusion $^{40}\text{Ar}/^{39}\text{Ar}$ dating of Bed I, Olduvai Gorge, Tanzania. *Nature* **354**, 145–149 (1991).
28. Manega, P.C. *Geochronology, geochemistry, and isotopic study of Plio-Pleistocene hominid sites and the Ngorongoro volcanic highlands in northern Tanzania*. (Ph.D Dissertation, University of Colorado, 1993).